Low-frequency fluctuation regime in a multimode semiconductor laser subject to a mode-selective optical feedback

F. Rogister, M. Sciamanna, O. Deparis, P. Mégret, and M. Blondel
Advanced Research in Optics, Service d'Electromagnétisme et de Télécommunications, Faculté Polytechnique de Mons, 31 Boulevard Dolez, B-7000 Mons, Belgium
(Received 16 July 2001; published 10 December 2001)

We study numerically the dynamics of a multimode laser diode subject to a mode-selective optical feedback by using a generalization of the Lang-Kobayashi equations. In this configuration, only one longitudinal mode of the laser is reinjected into the laser cavity; the other modes are free. When the laser operates in the low-frequency fluctuation regime, our model predicts intensity bursts in the free modes simultaneously with dropouts in the selected mode, in good agreement with recent experiments. In the frame of our model, intensity bursts and dropouts are associated with collisions of the system trajectory in phase space with saddle-type antimodes.

DOI: 10.1103/PhysRevA.65.015602 PACS number(s): 42.65.Sf, 42.60.Mi, 42.55.Px

I. INTRODUCTION

Subject to external, delayed, optical feedback, laser diodes present a large variety of qualitatively different dynamical behaviors. Among them, the low-frequency fluctuation (LFF) regime consists of sudden dropouts in the laser intensity followed by gradual recoveries on a time scale much larger than the period of the relaxation oscillations or the external-cavity round-trip time [1]. A popular interpretation of the LFF phenomenon relies on the Lang-Kobayashi equations [2], which assume a single-mode operation of the laser and a weak or moderate amount of external optical feedback. According to this interpretation [3], the intensity dropouts are consecutive with collisions of the system trajectory in phase space with saddle-type antimodes. Each of these collisions is preceded by a chaotic itinerancy of the trajectory among the attractor ruins of external cavity modes, with a drift towards the maximum gain mode. Additional numerical investigations of the Lang-Kobayashi equations have anticipated the presence of irregular intensity pulses [4] that have been experimentally confirmed using a streak camera [5]. In experimental studies on the LFF regime, a frequency-selective optical component such as an etalon [6] or a grating [7] is often placed in the external cavity in order to fulfill the single-mode assumption of the Lang-Kobayashi equations. This device is adequately tuned so that only one longitudinal mode is selected and reinjected into the laser cavity. The other modes are not subjected to the optical feedback and are referred to in the following as the *free modes*. In this way, the laser is restricted to oscillate essentially in the *selected mode* [6,7]. However, the occurrence of intensity bursts in the free modes simultaneously with dropouts in the mode selected by the feedback has recently been reported in similar experimental arrangements [8,9]. A first heuristic interpretation of the intensity dropouts observed in the selected mode and the bursts in the free modes has been given by Giudici *et al.* [9] and is based on the reduced stability of the selected mode with regards to perturbations occurring in the free modes. More recently, relying on an adaptation of the Tang, Statz, and deMars equations [10] to a semiconductor laser [11], the selective mode-induced LFF has been interpreted to be associated with a heteroclinic connection between a saddle node and an unstable focus [12]. Moreover, in the frame of this model, chaotic itinerancy with a drift is not a possible mechanism as long as intensity bursts in the free modes are observed [12]. A question that deserves investigation is then the following: may the dynamical instability induced by a selective feedback still be related to the interpretation given by Sano for the conventional LFF? Since many of the techniques for controlling the LFF regime [7,13,14] are linked to the so-called chaotic itinerancy with a drift, answering this question is indeed an important issue.

In this Brief Report, we investigate numerically the LFF regime in a multimode laser diode subject to a mode-selective optical feedback by using an extension of the Lang-Kobayashi equations [15]. We demonstrate that this model predicts the occurrence of intensity bursts in the free modes simultaneously with dropouts in the selected mode. We interpret the intensity bursts in the free modes to be associated with brusque increases of the carrier population that take place as the selected mode intensity drops. We finally show that LFF induced by the mode-selective feedback may still be associated with collisions of the system trajectory with saddle-type antimodes and chaotic itinerancies with a drift.

II. MULTIMODE RATE EQUATIONS

We have used in Ref. [15], a multimode extension of the Lang-Kobayashi equations for the slowly varying modal complex electric fields and carrier number that takes into account spontaneous emission noise and assumes a parabolic gain profile. These are equivalent to the following set of equations expressed in terms of the photon number and the electric-field phase in each longitudinal mode, and the carrier number, respectively, P_m, ϕ_m, and N where m is the mode number:

$$\frac{dP_m}{dt}=[G_m(N)-\gamma_m]P_m+\frac{2\kappa_m}{\tau_{\mathrm{Lm}}}\sqrt{P_m(t)P_m(t-\tau)}\times\cos[\phi_m(t)-\phi_m(t-\tau)+\omega_m\tau]+R_{\mathrm{sp}}, \qquad (1)$$

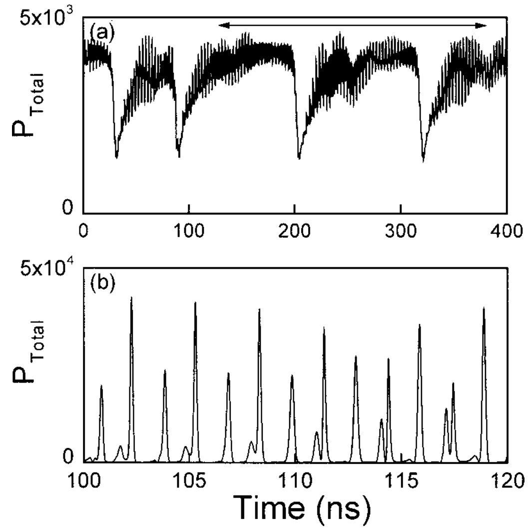

FIG. 1. (a) Time trace of the laser total intensity. The trace has been averaged over 2 ns. (b) Time trace of the unaveraged total number of photons emitted by the laser.

$$\frac{d\phi_m}{dt}=\frac{\alpha}{2}[G_m(N)-\gamma_m]-\frac{\kappa_m}{\tau_{Lm}}\sqrt{\frac{P_m(t-\tau)}{P_m(t)}}\times\sin[\phi_m(t)-\phi_m(t-\tau)+\omega_m\tau], \tag{2}$$

$$\frac{dN}{dt}=\frac{I}{e}-\frac{N}{\tau_S}-\sum_m G_m(N)P_m, \tag{3}$$

with

$$G_m(N)=G_c(N-N_0)\left[1-(m-m_c)^2\left(\frac{\Delta\omega_L}{\Delta\omega_g}\right)^2\right]. \tag{4}$$

α is the linewidth enhancement factor, G_m and γ_m are the mode-dependent gain coefficient and cavity loss. τ is the round-trip time in the external cavity. τ_{Lm} is the round-trip time of the mth optical mode inside the diode cavity. $\omega_m\tau$ and κ_m are, respectively, the feedback phase and the feedback level of the mth mode. In our study, $\kappa_m \equiv \kappa\delta_{mn}$ where n is the index of the mode that is selected and reinjected into the laser cavity. I is the injection current and I_{th} the threshold current of the solitary laser. e is the magnitude of the electron charge. τ_s is the lifetime of electron-hole pairs. N_0 is the transparency value of N. G_c and m_c are the gain coefficient and the longitudinal mode number at the gain peak. $\Delta\omega_L$ and $\Delta\omega_g$ are the longitudinal mode spacing and the gain width of the laser material, respectively. In the model, spontaneous emission is taken into account by means of the term R_{sp} that is the mean spontaneous emission rate. Stochastic fluctuations arising from spontaneous emission process are, however, neglected. In our calculations, we assume seven active optical modes and that γ_m is mode independent. The parabolic gain profile is centered on the fourth longitudinal mode. In this study, we choose the third longitudinal mode to be the one that is selected and fed back into the laser. The dynamical behavior of the laser remains qualitatively the same regardless of the mode selected. The laser parameters

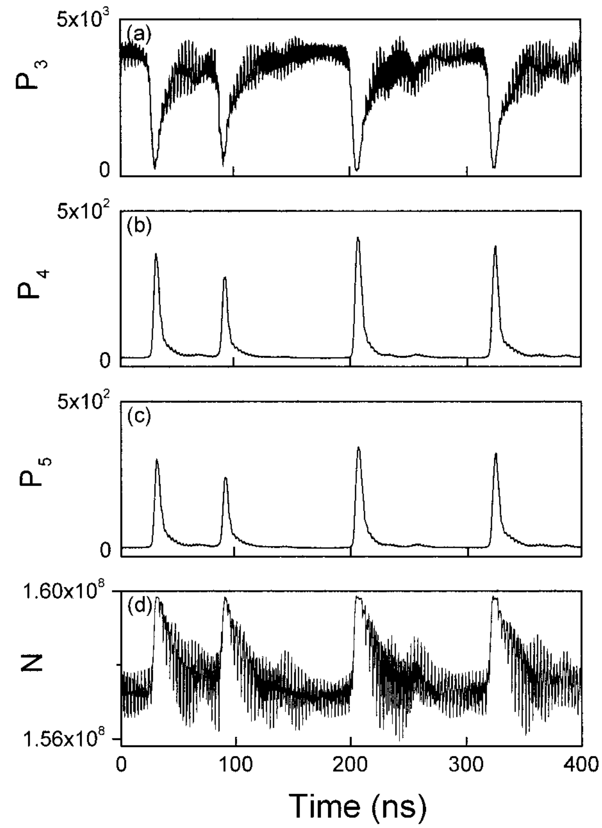

FIG. 2. Time traces of the intensity of mode 3 [selected mode, trace (a)], modes 4 and 5 [free modes, traces (b)–(c)], and time trace of the carrier number [trace (d)]. Traces (a)–(d) have been averaged over 2 ns.

are $\alpha=4$, $\gamma_m=5\times10^{11}\,\text{s}^{-1}$, $\tau_s=2$ ns, $G_c=1\times10^4\,\text{s}^{-1}$, $m_c=4$, $n=3$, $N_0=1.1\times10^8$, $R_{\text{sp}}=1.1\times10^{12}\,\text{s}^{-1}$, $\Delta\omega_g=2\pi\times4.7$ THz, and $\Delta\omega_L=2\pi/\tau_{Lm}$ with $\tau_{Lm}=8$ ps.

III. NUMERICAL RESULTS

The LFF regime may be observed in a large range of feedback parameters when the injection current is close to its threshold value. Here, we choose $I=1.0125\times I_{\text{th}}$, $\kappa=0.12$, $\tau=3$ ns, and the feedback phase in the selected mode $\omega_3\tau=0$. Figure 1(a) displays the total intensity averaged over 2 ns to model the limited bandwidth of detectors that are usually employed in experiments. The average total intensity increases steadily with time until it reaches a plateau and finally drops. After the dropout, the intensity gradually recovers until it drops again. On a picosecond time scale, the total intensity exhibits trains of fast pulses [Fig. 1(b)] that are approximately 150 ps wide and distant of about 1.5 ns. Between two consecutive pulses, the laser intensity is nearly zero. Figure 2 presents the evolution of the modal intensities and the carrier number underlying the total intensity behavior shown in Fig. 1(a). The traces (a)–(c) show the temporal evolution of the averaged intensities in the selected mode $(m=3)$, in the central mode $(m=4)$, and in a side mode $(m=5)$, respectively. The trace (d) shows the behavior of

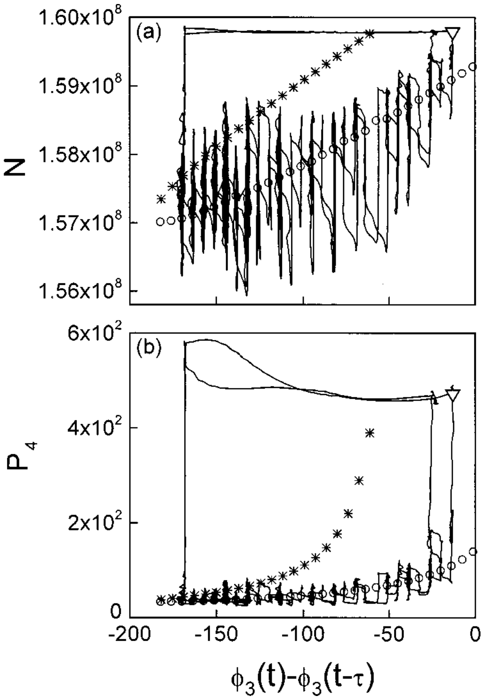

FIG. 3. (a),(b) Projection of the system trajectory onto the $[\phi_3(t)-\phi_3(t-\tau),N(t)]$ and $[\phi_3(t)-\phi_3(t-\tau),P_4(t)]$ planes. Circles (○) and stars represent, respectively, the projections of external cavity modes and antimodes. The sign ▽ identifies the solitary laser steady state. The trajectory is plotted for two consecutive dropouts and corresponds to the time interval indicated by the arrow in Fig. 1(a).

the unaveraged carrier number. Similar to the total intensity, sudden dropouts followed by long recoveries are observed in the selected mode [Fig. 2(a)]. In good agreement with experiments [8,9], the free modes that are depressed most of the time present bursts simultaneously with the dropouts in the selected mode [Figs. 2(b),2(c)]. The simultaneity of dropouts and bursts is easily checked by comparing the time trace of the total intensity [Fig. 1(a)] with the trace of the selected mode [Fig. 2(a)]: the dropouts in the selected mode are more pronounced than those of the total intensity. The occurrence of bursts in the free modes simultaneously with dropouts in the selected mode may be interpreted as follows. The selected mode plays the central role. The brusque increases of the population inversion [Fig. 2(d)] that are associated with the intensity dropouts in the selected mode lead the free modes, triggered by spontaneous emission, to lase during a short time. The bursts last until the carrier number begins to fall. It is important to notice at this point that spontaneous emission is necessary to observe the bursts. If the mean spontaneous emission rate is set to zero, i.e., $R_{\mathrm{sp}}=0$, the free modes die off after a short transient.

Steady-state solutions of the rate equations are zeros of the system of nonlinear transcendental algebraic equations obtained by substituting $P_m(t)=P_{\mathrm{sm}}$, $\phi_m(t)=(\omega_{\mathrm{sm}}-\omega_m)t$ and $N(t)=N_s$ in Eqs. (1)–(3). They are numerically found by using a Newton-Raphson zero-finding algorithm. Similar to the case of single-mode Lang-Kobayashi equations [2], steady-state solutions of Eqs. (1)–(3) are created by pairs through saddle-node bifurcations as the feedback level increases (not shown). Of each pair of steady-state solutions, one is a saddle point and is referred to as antimode. We refer to the other one as the external-cavity mode. Figure 3 shows the projection of the system trajectory, the steady-state solutions of Eqs. (1)–(3), as well as the steady-state solution that corresponds to the solitary laser (i.e., in the absence of feedback) onto the $[\phi_3(t)-\phi_3(t-\tau), N(t)]$ and $[\phi_3(t)-\phi_3(t-\tau), P_4(t)]$ planes. Figure 3 reveals that the system trajectory displays a chaotic itinerancy among the external-cavity modes with a drift towards the maximum gain mode close to which collisions with saddle-type antimodes occur. Just after the collision, the trajectory is repelled towards higher values of both the carrier number [Fig. 3(a)] and the free mode intensities [Fig. 3(b)], while the intensity in the selected mode drops (not shown). The laser then relaxes to its solitary state. The delayed feedback on the selected mode triggers the system and the chaotic itinerancy then restarts.

IV. CONCLUSIONS

In conclusion, we have numerically studied the dynamics of a multimode laser diode subject to a mode-selective optical feedback and operating in the low-frequency fluctuation regime. In good agreement with recent experiments, the multimode extension of the Lang-Kobayashi equations we have used predicts intensity bursts in the free modes simultaneously with dropouts in the selected mode. Bursts in the free modes and dropouts in the selected mode are found to be associated with collisions of the system trajectory in phase space with saddle-type antimodes preceded by a chaotic itinerancy of the system among external-cavity modes.

Relating the interpretation of the LFF regime in laser diodes subject to global optical feedback (with synchronous dropouts in each mode) to the conventional interpretation of Sano for the single-mode LFF is the next important issue that could gain insight from the results we have presented here.

ACKNOWLEDGMENTS

This work was funded by the Inter-University Attraction Pole Program (IAP IV 07) of the Belgian government and the Fonds National de la Recherche Scientifique.

[1] C. Risch and C. Voumard, J. Appl. Phys. **48**, 2083 (1977).
[2] R. Lang and K. Kobayashi, IEEE J. Quantum Electron. **QE-16**, 347 (1980).
[3] T. Sano, Phys. Rev. A **50**, 2719 (1994).
[4] G. H. M. van Tartwijk, A. M. Levine, and D. Lenstra, IEEE J. Sel. Top. Quantum Electron. **1**, 466 (1995).
[5] I. Fischer, G. H. M. van Tartwijk, A. M. Levine, W. Elsässer, E. Göbel, and D. Lenstra, Phys. Rev. Lett. **76**, 220 (1996).
[6] T. Heil, I. Fischer, and W. Elsäßer, Phys. Rev. A **58**, R2672 (1998).

[7] F. Rogister, D. W. Sukow, A. Gavrielides, P. Mégret, O. Deparis, and M. Blondel, Opt. Lett. **25**, 808 (2000).
[8] G. Huyet, S. Balle, M. Giudici, C. Green, G. Giacomelli, and J. R. Tredicce, Opt. Commun. **149**, 341 (1998).
[9] M. Giudici, L. Giuggioli, C. Green, and J. R. Tredicce, Chaos, Solitons Fractals **10**, 811 (1999).
[10] C. L. Tang, H. Statz, and G. deMars, J. Appl. Phys. **34**, 2289 (1963).
[11] H. Statz, C. L. Tang, and J. M. Lavine, J. Appl. Phys. **35**, 2581 (1964).
[12] E. A. Viktorov and P. Mandel, Opt. Lett. **25**, 1576 (2000).
[13] T. Heil, I. Fischer, and W. Elsäßer, Phys. Rev. A **60**, 634 (1999).
[14] D. Sukow and D. J. Gauthier, IEEE J. Quantum Electron. **36**, 175 (2000).
[15] F. Rogister, P. Mégret, O. Deparis, and M. Blondel, Phys. Rev. A **62**, 061803(R) (2000).